

Piezoelectric properties of Ga₂O₃: a first-principle study

San-Dong Guo and Hui-Min Du

School of Electronic Engineering, Xi'an University of Posts and Telecommunications, Xi'an 710121, China

The compounds exhibit piezoelectricity, which demands to break inversion symmetry, and then to be a semiconductor. For Ga₂O₃, the orthorhombic case (ϵ -Ga₂O₃) of common five phases breaks inversion symmetry. Here, the piezoelectric tensor of ϵ -Ga₂O₃ is reported by using density functional perturbation theory (DFPT). To confirm semiconducting properties of ϵ -Ga₂O₃, its electronic structures are studied by using generalized gradient approximation (GGA) and Tran and Blaha's modified Becke and Johnson (mBJ) exchange potential. The gap value of 4.66 eV is predicted with mBJ method, along with the effective mass tensor for electrons at the conduction band minimum (CBM) [about 0.24 m_0]. The mBJ gap is very close to the available experimental value. The elastic tensor C_{ij} and piezoelectric stress tensor e_{ij} are attained by DFPT, and then piezoelectric strain tensor d_{ij} are calculated from C_{ij} and e_{ij} . In this process, average mechanical properties of ϵ -Ga₂O₃ are estimated, such as bulk modulus, Shear modulus, Young's modulus and so on. The calculated d_{ij} are comparable and even higher than commonly used piezoelectric materials such as α -quartz, ZnO, AlN and GaN.

PACS numbers: 71.20.-b, 77.65.-j, 77.65.Bn

Email:sandongyuwang@163.com

Keywords: Piezoelectricity, Energy gap, Elastic constants, Gallium oxide

I. INTRODUCTION

Wide-band gap semiconductors have potential application in high-power electronics, which requires high frequency, temperature and power. Gallium oxide (Ga₂O₃) has received a lot of attention as a wide band gap transparent semiconducting oxide¹⁻⁶. The Ga₂O₃ has five different phases, commonly referred to as α , β , γ , δ and ϵ , the monoclinic β phase of which is the most thermodynamically stable with the energy gap 4.6-4.9 eV, transparency up to the UV-C range, and very high breakdown voltage^{1,3}. Piezoelectric materials can convert mechanical energy to electrical energy, which have potential application in sensors and energy harvesting⁷. The ZnO, GaN and InN semiconductors with non-centrosymmetric wurtzite-structure are widely used in the piezotronic and piezo-phototronic devices, and their nanostructures have potential applications in electromechanical coupled sensors and nanoscale energy conversion⁸⁻¹¹.

For piezoelectric materials, inversion symmetry need be eliminated. The bravais lattice, space group, point group and inversion center of five different polymorphs of Ga₂O₃ are shown in Table I. It is clearly seen that ϵ -Ga₂O₃ breaks inversion symmetry and hence can exhibit piezoelectricity. The ϵ -phase of Ga₂O₃ is confirmed as the second most stable structure after β -Ga₂O₃¹². When ϵ -Ga₂O₃ is epitaxially stabilized, the symmetry will prevent the transform back into β -phase. The electronic structures of ϵ -Ga₂O₃ have been reported, and the predicted gap is 2.465 eV with GGA¹³, 2.32 eV with PBEsol, 4.62 eV with B3LYP¹⁴ and 4.26 eV with HSE¹⁵. The experimental gap is 4.41 eV by angle-resolved photoemission spectroscopy (ARPES) experiments¹⁵, and is 4.6 eV from photoconductivity and optical absorption¹⁶. The ϵ -Ga₂O₃ is predicted to have a large spontaneous polarization (0.23-0.26 C/m²)^{12,14}, along with piezoelectric coefficient $e_{33}=0.77$ C/m²¹². Recently, piezoelectric strain

TABLE I. The bravais lattice, space group, point group and inversion center of five different polymorphs of Ga₂O₃.

Name	α	β	γ	δ	ϵ
Bravais lattice	Trigonal	Monocl.	Cubic	Cubic	Orthorh.
Space group	$R\bar{3}c$	$C2/m$	$Fd\bar{3}m$	$Ia\bar{3}$	$Pna2_1$
Point group	$\bar{3}m$	$2/m$	$m\bar{3}m$	$m\bar{3}$	$mm2$
Inversion center	\checkmark	\checkmark	\checkmark	\checkmark	\times

constants (d_{ij}) of ϵ -Ga₂O₃ are calculated from piezoelectric stress constants (e_{ij}) and elastic constants (C_{ij})¹⁷. The e_{ij} are attained by polarization-strain relation, and the C_{ij} are calculated by energy-strain relation¹⁷. Here, we use DFPT to attain the C_{ij} and e_{ij} , and then calculate the d_{ij} by e matrix multiplying C matrix inversion. To ensure the reliability of our results, the piezoelectric properties of commonly used piezoelectric materials such as ZnO, AlN and GaN are also studied by DFPT, and make a comparison with the related experiments¹⁸⁻²². The mBJ is used to study the electronic structures of ϵ -Ga₂O₃, and the calculated mBJ gap 4.66 eV is very close to experimental values^{15,16}. The mBJ is as cheap as local density approximation (LDA) or GGA, thus can be used to study very large systems such as doping ϵ -Ga₂O₃ in an efficient way.

II. SYMMETRY ANALYSIS

The piezoelectric effect is an electromechanical coupling described by piezoelectric tensors e_{ijk} and d_{ijk} , which are obtained as the sum of ionic and electronic contributions. In the following, the frequently used Voigt notation is employed, and the mapping of indices is 11 \rightarrow 1, 22 \rightarrow 2, 33 \rightarrow 3, 23 \rightarrow 4, 31 \rightarrow 5 and 12 \rightarrow 6. The Voigt notation allows to represent the tensor of elastic constants

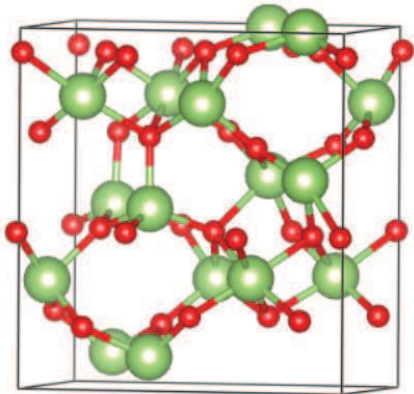


FIG. 1. (Color online) The crystal structure of ϵ -Ga₂O₃. The large green balls represent Ga atoms, and the small red balls for O atoms.

C_{ijkl} , piezoelectric tensors e_{ijk} and d_{ijk} as 6×6 , 3×6 and 3×6 matrix C_{ij} , e_{ij} and d_{ij} , with a maximum of 21, 18 and 18 independent elements. The number of independent components can be reduced due to the crystal symmetry in C_{ij} , e_{ij} and d_{ij} tensors. The ϵ -Ga₂O₃ has the $mm2$ point group symmetry, giving:

$$e = \begin{pmatrix} 0 & 0 & 0 & 0 & e_{15} & 0 \\ 0 & 0 & 0 & e_{24} & 0 & 0 \\ e_{31} & e_{32} & e_{33} & 0 & 0 & 0 \end{pmatrix} \quad (1)$$

$$C = \begin{pmatrix} C_{11} & C_{12} & C_{13} & 0 & 0 & 0 \\ C_{12} & C_{22} & C_{23} & 0 & 0 & 0 \\ C_{13} & C_{23} & C_{33} & 0 & 0 & 0 \\ 0 & 0 & 0 & C_{44} & 0 & 0 \\ 0 & 0 & 0 & 0 & C_{55} & 0 \\ 0 & 0 & 0 & 0 & 0 & C_{66} \end{pmatrix} \quad (2)$$

The elastic tensor C_{ij} and piezoelectric stress tensor e_{ij} can be attained by density functional theory (DFT) calculations, and the piezoelectric strain tensor d_{ij} can be calculated by the relation:

$$e = dC \quad (3)$$

and

$$d = \begin{pmatrix} 0 & 0 & 0 & 0 & d_{15} & 0 \\ 0 & 0 & 0 & d_{24} & 0 & 0 \\ d_{31} & d_{32} & d_{33} & 0 & 0 & 0 \end{pmatrix} \quad (4)$$

III. ELECTRONIC STRUCTURES

The crystal structure of ϵ -Ga₂O₃ has 16 (24) Ga (O) atoms at four (six) different Wyckoff positions 4a,

TABLE II. The atomic coordinates of ϵ -Ga₂O₃ with $a=5.06$ Å, $b=8.69$ Å and $c=9.30$ Å.

atom	x	y	z
Ga1	0.18017	0.15153	0.99762
Ga2	0.81334	0.16181	0.30879
Ga3	0.19165	0.15083	0.58692
Ga4	0.67799	0.03128	0.79570
O1	0.97429	0.32590	0.42764
O2	0.52161	0.48778	0.43308
O3	0.65030	0.00345	0.20151
O4	0.15460	0.15917	0.19757
O5	0.84997	0.17145	0.67252
O6	0.52301	0.16682	0.93836

which is plotted in Figure 1. Within the DFT²³, a full-potential linearized augmented-plane-waves method is used to investigate electronic structures of Ga₂O₃ by using WIEN2k code²⁴. We use Tran and Blaha's mBJ approach for the exchange potential (plus LDA correlation potential)²⁵, and the popular GGA of Perdew, Burke and Ernzerhof (GGA-PBE)²⁶ to do comparative studies. We use a $12 \times 7 \times 6$ k-point meshes in the first Brillouin zone (BZ) for the self-consistent calculation, make harmonic expansion up to $l_{\max} = 10$ in each of the atomic spheres, and set $R_{\text{mt}} * k_{\max} = 8$.

The optimized structure-related data are summarized in Table II by using GGA, which agree well with previous calculated values¹³. Firstly, the popular GGA is used to perform the self-consistent calculation, and the improved exchange-correlation functional including the mBJ exchange potential is adopted, which can improve the semiconductor gaps and d state positions for many kinds of materials. The energy bands calculated with GGA and mBJ are presented in Figure 2. The GGA gap value is 2.45 eV, and 4.66 eV for mBJ functional. Our GGA gap accords with other GGA value 2.465 eV¹³. The mBJ gap is very close to HSE one (4.26 eV)¹⁵ and B3LYP one (4.62 eV)¹⁴, and is also close to experimental value 4.41 eV by ARPES experiments¹⁵ and 4.6 eV indicated by photoconductivity and optical absorption¹⁶. Both GGA and mBJ results show a CBM at the G point. A quasi-direct gap is observed with the valence band maximum (VBM) is a bit off G in the G-X direction. The energy difference between G point and VBM only is 1.2 meV with GGA and 0.2 meV with mBJ. The experimental data suggest that the VBM is at or near the zone centre¹⁵. The experimental gap for β -Ga₂O₃ has been reported in the range of 4.6-4.9 eV^{1,3}. The mBJ is used to study the electronic structures of β -Ga₂O₃ ($a=12.29$ Å, $b=3.05$ Å, $c=5.81$ Å and $\beta=103.77$). The mBJ gap value of β -Ga₂O₃ is 4.61 eV, which shows that mBJ can reproduce the gap of Ga₂O₃ very well. We also determine the effective mass tensor for electrons at the CBM, and the resulting results in units of the free electron mass m_0 are: $m_{xx}=0.237$, and $m_{yy}=m_{zz}=0.235$, which shows that

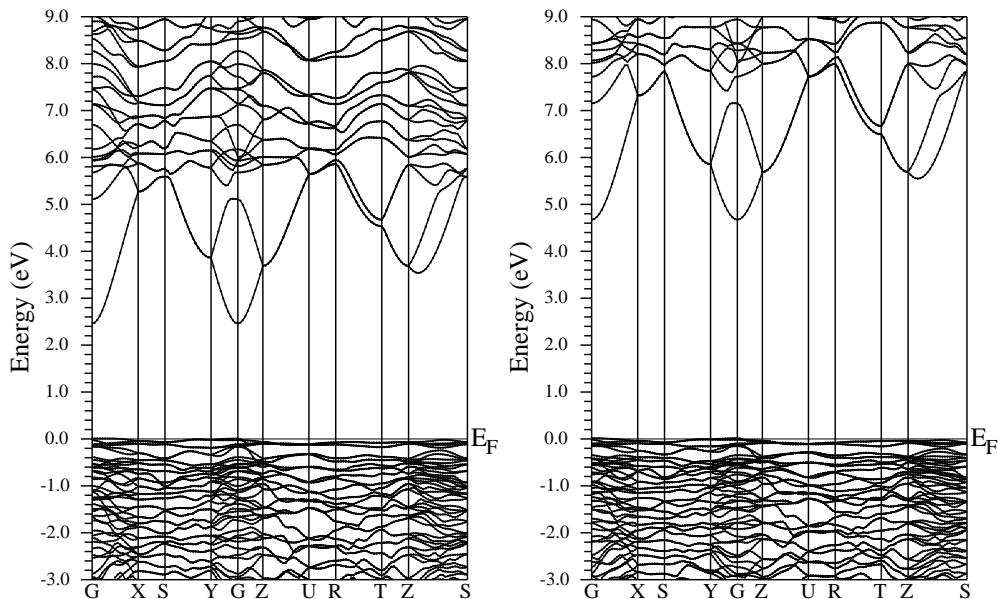


FIG. 2. The energy band structures of ϵ -Ga₂O₃ using GGA (Left) and mBJ (Right).

TABLE III. For ϵ -Ga₂O₃, bulk modulus (B), Shear modulus (G), Young's modulus (E), Poisson's ratio (ν), longitudinal wave velocity (v_l), transverse wave velocity (v_t), average wave velocity (v_a) and Debye temperature (Θ_D).

B (GPa)	G (GPa)	E (GPa)	ν
209.22	82.50	218.75	0.33
v_l (km/s)	v_t (km/s)	v_a (km/s)	Θ_D (K)
7.24	3.68	4.12	565.81

the anisotropy is rather small. These effective masses are very close to ones of monoclinic and rhombohedral cases¹³.

TABLE IV. The elastic constants C_{ij} of ZnO, AlN and GaN, and the unit is GPa.

Name	C_{11}	C_{12}	C_{13}	C_{33}	C_{44}
ZnO	204.3	133.2	115.8	209.3	34.3
AlN	392.0	141.6	105.5	372.2	112.5
GaN	344.8	133.4	93.9	379.6	89.6

IV. PIEZOELECTRIC PROPERTIES

The elastic tensor C_{ij} and piezoelectric stress tensor e_{ij} are obtained by using DFPT²⁷ as implemented in VASP code²⁸⁻³⁰. The relaxed-ion elastic tensor and piezoelectric stress tensor are obtained from the sum of ionic and electronic contributions. Within DFPT, the electronic and ionic contributions to the piezoelectric tensor can be calculated directly in the VASP code. A $12 \times 7 \times 6$ k-point

mesh is used, and the exchange-correlation interactions are treated using the GGA-PBE with a kinetic-energy cutoff of 450 eV. It is noted that the order of indices in VASP code is 1(XX), 2(Y Y), 3(ZZ), 6(XY), 4(YZ), 5(ZX), and we have changed into the normal order in the following results for elastic and piezoelectric tensors. The elastic tensor C_{ij} are given (in GPa):

$$\begin{pmatrix} 354.77 & 165.45 & 142.20 & 0 & 0 & 0 \\ 165.45 & 316.08 & 150.21 & 0 & 0 & 0 \\ 142.20 & 150.21 & 302.61 & 0 & 0 & 0 \\ 0 & 0 & 0 & 82.75 & 0 & 0 \\ 0 & 0 & 0 & 0 & 61.75 & 0 \\ 0 & 0 & 0 & 0 & 0 & 102.61 \end{pmatrix} \quad (5)$$

Based on C_{ij} , average mechanical properties of ϵ -Ga₂O₃ can be attained, including bulk modulus, Shear modulus, Young's modulus, Poisson's ratio, longitudinal wave velocity, transverse wave velocity, average wave velocity and Debye temperature. The Born criteria of mechanical stability for an orthorhombic crystal is³¹:

$$C_{11} > 0, C_{44} > 0, C_{55} > 0, C_{66} > 0 \quad (6)$$

$$C_{11}C_{22} > C_{12}^2 \quad (7)$$

$$C_{11}C_{22}C_{33} + 2C_{12}C_{13}C_{23} - C_{11}C_{23}^2 - C_{22}C_{13}^2 - C_{33}C_{12}^2 > 0 \quad (8)$$

The calculated C_{ij} satisfy these conditions, proving that that ϵ -Ga₂O₃ is mechanically stable. The related data are summarized in Table III. The bulk (shear) modulus B (G) manifests the resistance to fracture (plastic deformation). A high (low) B/G ratio may indicates its

TABLE V. Piezoelectric coefficients $e_{ij}(d_{ij})$ of ZnO, AlN and GaN, and the unit is C/m² (pm/V). The related experimental values of ZnO¹⁸, AlN¹⁹ and GaN¹⁹⁻²² are shown in parentheses.

Name	e_{33}	e_{31}	e_{15}	d_{33}	d_{31}	d_{15}
ZnO	1.33 (0.96)	-0.65 (-0.62)	-0.49 (-0.37)	13.63 (12.3)	-6.59 (-5.1)	-14.20 (-8.3)
AlN	1.61 (1.55)	-0.65 (-0.58)	-0.34 (-0.48)	5.65 (5.53)	-2.34 (-2.65)	-3.00 (-4.07)
GaN	0.67 (1.00 ¹⁹)	-0.37 (-0.36 ¹⁹)	-0.23 (-0.30 ¹⁹)	2.38 (3.1 ²⁰)	-1.24 (-1.0 ²¹)	-2.52 (-3.1 ²²)

ductility (brittleness), and the critical value is around 1.75, which can be used to separate ductile and brittle materials. The value of ϵ -Ga₂O₃ is 2.54, and it can be classified as a ductility material.

The piezoelectric stress tensor e_{ij} are shown (in C/m²):

$$\begin{pmatrix} 0 & 0 & 0 & 0 & 0.595 & 0 \\ 0 & 0 & 0 & 0.194 & 0 & 0 \\ 0.011 & -0.319 & 0.941 & 0 & 0 & 0 \end{pmatrix} \quad (9)$$

The piezoelectric strain tensor d_{ij} are derived by Equation 3, giving (in pm/V):

$$\begin{pmatrix} 0 & 0 & 0 & 0 & 9.622 & 0 \\ 0 & 0 & 0 & 2.345 & 0 & 0 \\ -0.489 & -3.060 & 4.858 & 0 & 0 & 0 \end{pmatrix} \quad (10)$$

The ϵ -Ga₂O₃ possesses five independent components of the piezoelectric tensor, namely d_{31} , d_{32} , d_{33} , d_{15} and d_{24} . The magnitudes of d_{ij} range from 0.489 pm/V to 9.622 pm/V, the d_{33} and d_{15} of which are comparable and even higher than commonly used piezoelectric materials such as α -quartz, ZnO, AlN and GaN^{18-22,32}. We note that d_{31} is smaller by 1 order of magnitude compared to other d_{ij} , which is due to very small e_{31} . The d_{15} is the largest among the d_{ij} , which is due to the large e_{15} and the smallest C_{55} ($d_{15}=e_{15}/C_{55}$). Our calculated d_{ij} are close to previous theoretical values ($d_{32}=-3.43$ pm/V, $d_{33}=4.06$ pm/V, $d_{24}=2.69$ pm/V, $d_{15}=14.60$ pm/V) except d_{31} (1.37 pm/V)¹⁷. In previous calculations, the elastic tensor C_{ij} are attained by fitting the DFT-calculated unit-cell energy to a series of strain states, and the piezoelectric stress tensor e_{ij} are calculated by evaluating the change of unit-cell polarization after imposing small strain¹⁷. Here, these tensors are calculated by DFPT. To ensure the reliability of our results or method, the piezoelectric properties of ZnO, AlN and GaN with $P6_3mc$ space group are also studied by DFPT. Due to $6mm$ point group of $P6_3mc$, they have five independent elastic constants (C_{11} , C_{12} , C_{13} , C_{33} and C_{44}), and three piezoelectric constants (e/d_{31} , e/d_{33} and e/d_{15}). The elastic constants of ZnO, AlN and GaN are shown in Table IV, which agree well with previous calculated values³³. The piezoelectric tensors of ZnO, AlN and

GaN are summarized in Table V, along with the related experimental values of ZnO¹⁸, AlN¹⁹ and GaN¹⁹⁻²². Our calculated piezoelectric tensors of ZnO, AlN and GaN are in reasonable agreement with experiments. The deviation may be because the related experiments are carried out on constrained epitaxial samples. Thus, our predicted piezoelectric tensors of ϵ -Ga₂O₃ should be receivable.

V. DISCUSSIONS AND CONCLUSION

It is clear that mBJ gives much better energy gap of ϵ -Ga₂O₃ than GGA toward the experimental values. Although HSE or B3LYP also can give reasonable energy gap, they need more CPU time and memory than mBJ. Thus, mBJ may be more suitable for dopant studies of ϵ -Ga₂O₃. It is noted that the energy gap and the effective masses (at CBM) of ϵ -Ga₂O₃ are very close to ones of β case, but ϵ phase shows good piezoelectric properties, which can add more freedom for electronic devices.

In summary, the electronic structures have been studied by GGA and mBJ, and the elastic and piezoelectric tensors are attained by DFPT. The mBJ gap is consistent with previously calculated HSE or B3LYP one, and has very better agreement with experiment than GGA one. The values of d_{ij} are found to be comparable to or even superior than conventional piezoelectric materials such as α -quartz, ZnO, AlN and GaN. These results show the possibility of employing piezoelectric effects in ϵ -Ga₂O₃ for electronics and energy applications. Our works can stimulate further experimental works to study piezoelectric properties of ϵ -Ga₂O₃.

ACKNOWLEDGMENTS

This work is supported by the Natural Science Foundation of Shaanxi Provincial Department of Education (19JK0809). We are grateful to the Advanced Analysis and Computation Center of China University of Mining and Technology (CUMT) for the award of CPU hours and WIEN2k/VASP software to accomplish this work.

¹ S. J. Pearton, J. C. Yang, P. H. Cary, F. Ren, J. Kim, M. J. Tadjer and M. A. Mastro, Appl. Phys. Rev. **5**, 011301

(2018).

- ² S. Yoshioka, H. Hayashi, A. Kuwabara, F. Oba, K. Matsunaga and I. Tanaka, *J. Phys.: Condens. Matter* **19**, 346211 (2007).
- ³ S. J. Pearton, F. Ren, M. Tadjer and J. Kim, *J. Appl. Phys.* **124**, 220901 (2018).
- ⁴ N. Ueda, H. Hosono, R. Waseda and H. Kawazoe, *Appl. Phys. Lett.* **70**, 3561 (1997).
- ⁵ M. Orita, H. Ohta, M. Hirano and H. Hosono, *Appl. Phys. Lett.* **77**, 4166 (2000).
- ⁶ F. Ricci, F. Boschi, A. Baraldi, A. Filippetti, M. Higashiwaki, A. Kuramata, V. Fiorentini and R. Fornari, *J. Phys.: Condens. Matter* **28**, 224005 (2016).
- ⁷ K. A. Cook-Chennault, N. Thambi and A. M. Sastry, *Smart Mater. Struct.* **17**, 043001 (2008).
- ⁸ F. Bernardini, V. Fiorentini and D. Vanderbilt, *Phys. Rev. Lett.* **79**, 3958 (1997).
- ⁹ Z. L. Wang, *Adv. Mater.* **24**, 4632 (2012).
- ¹⁰ C. Pan, L. Dong, G. Zhu, S. Niu, R. Yu, Q. Yang, Y. Liu and Z. L. Wang, *Nat. Photonics* **7**, 752 (2013).
- ¹¹ S. Xu, Y. Qin, C. Xu, Y. Wei, R. Yang and Z. L. Wang, *Nat. Nanotechnol.* **5**, 366 (2010).
- ¹² M. B. Maccioni and V. Fiorentini, *Appl. Phys. Express* **9**, 041102 (2016).
- ¹³ J. Furthmüller and F. Bechstedt, *Phys. Rev. B* **93**, 115204 (2016).
- ¹⁴ J. Kim, D. Tahara, Y. Miura and B. G. Kim, *Appl. Phys. Express* **11**, 061101 (2018).
- ¹⁵ M. Mulazzi, F. Reichmann, A. Becker, W. M. Klesse, P. Alippi, V. Fiorentini, A. Parisini, M. Bosi and R. Fornari, *APL Mater.* **7**, 022522 (2019).
- ¹⁶ M. Pavesi, F. Fabbri, F. Boschi, G. Piacentini, A. Baraldi, M. Bosi, E. Gombia, A. Parisini and R. Fornari, *Mater. Chem. Phys.* **205**, 502 (2018).
- ¹⁷ K. Shimada, *Mater. Res. Express* **5**, 036502 (2018).
- ¹⁸ Landolt-Börnstein, O. Madelung (Ed.), New Series, Group III: Solid State Physics, Low Frequency Properties of Dielectric Crystals: Piezoelectric, Pyroelectric and Related Constants, vol. 29b, Springer, Berlin, 1993.
- ¹⁹ K. Tsubouchi and N. Mikoshiba, *IEEE Trans. Sonics Ultrason.* **SU-32**, 634 (1985).
- ²⁰ C. M. Lueng, H. L. Chang, C. Suya and C. L. Choy, *J. Appl. Phys.* **88**, 5360 (2000).
- ²¹ A. Hangleiter, F. Htzel, S. Lahmann and U. Rossow, *Appl. Phys. Lett.* **83**, 1169 (2003).
- ²² S. Muensit, E. M. Goldys and I. L. Guy, *Appl. Phys. Lett.* **75**, 3965 (1999).
- ²³ P. Hohenberg and W. Kohn, *Phys. Rev.* **136**, B864 (1964); W. Kohn and L. J. Sham, *Phys. Rev.* **140**, A1133 (1965).
- ²⁴ P. Blaha, K. Schwarz, G. K. H. Madsen, D. Kvasnicka and J. Luitz, WIEN2k, an Augmented Plane Wave + Local Orbitals Program for Calculating Crystal Properties (Karlheinz Schwarz Technische Universität Wien, Austria) 2001, ISBN 3-9501031-1-2
- ²⁵ F. Tran and P. Blaha, *Phys. Rev. Lett.* **102**, 226401 (2009).
- ²⁶ J. P. Perdew, K. Burke and M. Ernzerhof, *Phys. Rev. Lett.* **77**, 3865 (1996).
- ²⁷ X. Wu, D. Vanderbilt and D. R. Hamann, *Phys. Rev. B* **72**, 035105 (2005).
- ²⁸ G. Kresse, *J. Non-Cryst. Solids* **193**, 222 (1995).
- ²⁹ G. Kresse and J. Furthmüller, *Comput. Mater. Sci.* **6**, **15** (1996).
- ³⁰ G. Kresse and D. Joubert, *Phys. Rev. B* **59**, 1758 (1999).
- ³¹ F. Mouhat and F. X. Coudert, *Phys. Rev. B* **90**, 224104 (2014).
- ³² R. Bechmann, *Phys. Rev.* **110**, 1060 (1958).
- ³³ K. Shimada, *Jpn. J. Appl. Phys.* **45**, L358 (2006).